

## Research Article

# Effects of Carrier Frequency Offset, Timing Offset, and Channel Spread Factor on the Performance of Hexagonal Multicarrier Modulation Systems

**Kui Xu and Yuehong Shen**

*Institute of Communications Engineering, PLA University of Science and Technology, No. 2 Biaoying Road, Yudao Street, Nanjing 210007, China*

Correspondence should be addressed to Kui Xu, xiancheng\_2005@163.com

Received 17 May 2008; Revised 6 October 2008; Accepted 31 January 2009

Recommended by Mounir Ghogho

Hexagonal multicarrier modulation (HMM) system is the technique of choice to overcome the impact of time-frequency dispersive transmission channel. This paper examines the effects of insufficient synchronization (carrier frequency offset, timing offset) on the amplitude and phase of the demodulated symbol by using a projection receiver in hexagonal multicarrier modulation systems. Furthermore, effects of CFO, TO, and channel spread factor on the performance of signal-to-interference-plus-noise ratio (SINR) in hexagonal multicarrier modulation systems are further discussed. The exact SINR expression versus insufficient synchronization and channel spread factor is derived. Theoretical analysis shows that similar degradation on symbol amplitude and phase caused by insufficient synchronization is incurred as in traditional cyclic prefix orthogonal frequency-division multiplexing (CP-OFDM) transmission. Our theoretical analysis is confirmed by numerical simulations in a doubly dispersive (DD) channel with exponential delay power profile and U-shape Doppler power spectrum, showing that HMM systems outperform traditional CP-OFDM systems with respect to SINR against ISI/ICI caused by insufficient synchronization and doubly dispersive channel.

Copyright © 2009 K. Xu and Y. Shen. This is an open access article distributed under the Creative Commons Attribution License, which permits unrestricted use, distribution, and reproduction in any medium, provided the original work is properly cited.

## 1. Introduction

Multicarrier modulation (MCM) is a popular transmission scheme in which the data stream is split into several substreams and transmitted, in parallel, on different subcarriers. We consider MCM over time-varying multipath propagation channels which spread the MCM signal simultaneously in both the time and frequency domains. This spreading induces both intersymbol interference (ISI) and intercarrier interference (ICI) which complicate data demodulation. We will refer to channels that are time dispersive and frequency dispersive as doubly dispersive (DD) channels.

Orthogonal frequency-division multiplexing (OFDM) systems with guard time interval or cyclic prefix can prevent ISI, but do not combat ICI because they are based on rectangular-type pulses. In order to overcome the aforementioned drawbacks of OFDM systems, several pulse-shaping OFDM systems were proposed [1–15]. Most works on pulse design exclusively dealt with rectangular time-frequency

(TF) lattices. It is shown that transmission in rectangular lattices is suboptimal for doubly dispersive channels [9]. By using sphere covering theory, the authors have demonstrated that lattice OFDM (LOFDM) systems, which are OFDM systems based on hexagonal-type lattices, provide better performance against ISI/ICI. However, LOFDM confines the transmission pulses to a set of orthogonal ones. As pointed out in [2, 10, 13, 16], these orthogonalized pulses destroy the time-frequency (TF) concentration of the initial pulses, hence lower the robustness to the time and frequency dispersion caused by the propagation channel.

In [16], the authors abandoned the orthogonality condition of the modulated pulses and proposed a multicarrier transmission scheme on hexagonal lattice named as hexagonal multicarrier modulation (HMM) by regarding signal transmission as tiling of the TF plane. To optimally combat the impact of the propagation channels, the lattice parameters and the pulse shape of modulation waveform are jointly optimized to adapt to the channel scattering function.

It is shown that the hexagonal multicarrier transmission systems obtain lower energy perturbation, hence outperform OFDM and LOFDM systems from the robustness against channel dispersion point of view.

Synchronization is considered as a key factor of designing multicarrier modulation system receiver. The synchronization precision significantly affects the receiver performance and usually depends on the precision of carrier frequency offset estimation and symbol timing. A generalized framework for the prediction of OFDM system performance in the presence of carrier frequency offset (CFO) and timing offset (TO), including the transmitter and receiver pulse shapes as well as the channel, is presented in [17]. The signal-to-interference-plus-noise ratio (SINR) performance low bound on the effects of Doppler spread in OFDM system is studied in [18].

In this paper, our attention is focused on the analysis of the effects of CFO and TO on the amplitude and phase of the demodulated symbol by using a straightforward but suboptimum projection receiver [2, 9, 10, 12, 13] in hexagonal multicarrier modulation systems. Furthermore, effects of CFO, TO, and channel spread factor on the performance of SINR in hexagonal multicarrier modulation systems are further discussed. The exact SINR expression versus CFO, TO, and channel spread factor is derived. Both theoretical analysis and simulation results show that similar degradation on symbol amplitude and phase caused by insufficient synchronization is incurred as in CP-OFDM transmission. Our theoretical analysis is confirmed by numerical simulations, showing that HMM systems outperform traditional CP-OFDM systems with respect to SINR against ISI/ICI caused by CFO, TO, and doubly dispersive channel.

## 2. Signal Transmission and TF Lattice

It is shown in [16, 19] that signal transmission can be viewed as tiling of the TF plane. In practice, almost all communication systems transmit the information symbols in a regular way, and the underlying tiling forms a lattice in the TF plane. In a nutshell, a *lattice*  $V$  in  $K$ -dimensional Euclidean space  $\mathbb{R}^K$  is a set of points arranged in a highly regular manner. Since we consider the signal transmission in the TF plane in this correspondence, we only confine our attention to two-dimensional (2D) case.

Specifically, in OFDM system with symbol period  $T$  and subcarrier separation  $F$ , the transmission functions of OFDM system consist of translations and modulations of a single prototype  $g(t)$ , which constitute a Weyl-Heisenberg system and create a 2D rectangular lattice with generator matrix

$$\mathbf{V} = \begin{bmatrix} T & 0 \\ 0 & F \end{bmatrix}. \quad (1)$$

Conventional time-division multiplex (TDM) mode and frequency-division multiplex (FDM) mode can be viewed as transmission on a one-dimensional (1D) lattice along the time axis and frequency axis, with generators  $[T \ 0]^T$  and

$[F \ 0]^T$ , respectively, where the superscript  $(\cdot)^T$  represents the transpose.

The lattice density is given by  $\rho = 1/\sqrt{\det(\mathbf{V}^T\mathbf{V})}$ , where  $\det(\cdot)$  denotes the determinant. The quantity  $\rho$  corresponds to the symbol density in the TF plane, which was known as *signaling efficiency* to represent the number of symbols per second per hertz. For signal transmission with general transmission pattern  $\mathbf{V}$ , the transmitted signal can be expressed as

$$s(t) = \sum_{\mathbf{z}} c_{\mathbf{z}} g(t, \mathbf{V}\mathbf{z}), \quad (2)$$

where  $c_{\mathbf{z}}$  is the data symbol indexed by  $\mathbf{z}$ , which is usually taken from a specific signal constellation and assumed to be independent and identically distributed (i.i.d.) with zero mean and average power  $\sigma_c^2$ ;  $g(t, \mathbf{V}\mathbf{z})$  is the modulation pulse associated with  $c_{\mathbf{z}}$  and  $\mathbf{z} = [m, n]^T$ ,  $m \in \mathcal{M}$ ,  $n \in \mathcal{N}$ , while  $m$  and  $n$  can be regarded as the generalized time index and subcarrier index, respectively. Moreover,  $\mathcal{M}$  and  $\mathcal{N}$  denote the sets from which  $m$ ,  $n$  can be taken.

It is well known that when a signal is transmitted over mobile radio channel, the energy of one symbol data will spread out to neighboring symbols due to the time and frequency dispersion, which produces ISI/ICI and degrades the system performance. In the view of signal transmission on lattice in the TF plane, the system performance is mainly determined by two factors:

- (i) the time-frequency localization of pulse shape  $g(t)$ ;
- (ii) the distance between adjacent time-frequency lattice point.

A better TF-concentrated pulse would lead to more robustness against the energy leakage. It is obvious that the larger the distance, the less the perturbation among the transmitted symbols.

## 3. Hexagonal Multicarrier Transmission System [16]

It is well known that the Gaussian pulse

$$g^\sigma(t) = \left(\frac{2}{\sigma}\right)^{1/4} e^{-(\pi/\sigma)t^2} \quad (3)$$

has the best energy concentration in the sense that it achieves the equality in the Heisenberg uncertainty principle  $W_t W_f \geq 1/4\pi$ , where  $W_t^2$  and  $W_f^2$  are the centralized temporal and spectral second-order moments, respectively [20]. By the Heisenberg uncertainty principle, any signal cannot be arbitrarily concentrated in the time and frequency directions simultaneously, which suggests that they must occupy some area in the TF plane.

The product  $W_t W_f$  characterizes the energy concentration of a pulse in the TF plane. The smaller the value of  $W_t W_f$  is, the more concentrated the pulse will be. Hence,

the Gaussian pulse is the natural choice as modulation waveform, in an attempt to achieve minimum energy perturbation over TF dispersive channels. Note that the parameter  $\sigma$  determines the energy distribution of the Gaussian pulse in the time and frequency directions, respectively. To be more specific, we have  $\sigma = W_t/W_f$ .

The ambiguity function of prototype is defined by

$$\begin{aligned} A_{g^\sigma}(\tau, \nu) &= \int_{-\infty}^{\infty} g^\sigma(t) g^{\sigma*}(t - \tau) e^{-j2\pi\nu t} dt \\ &= e^{-(\pi/2)((1/\sigma)\tau^2 + \sigma\nu^2)} e^{-j\pi\tau\nu}, \end{aligned} \quad (4)$$

where  $(\cdot)^*$  denotes the complex conjugate. It can be viewed as the 2D correlation between  $g(t)$  and its shifted version by  $\tau$  in time and  $\nu$  in frequency in the TF plane. We can conclude from (4) that the ambiguity function of the Gaussian pulse is an ellipse in the TF plane.

As pointed out in [16], for a given signaling efficiency, the information-bearing pulses arranged on a hexagonal lattice can be separated as sufficiently as possible in the TF plane. An example of hexagonal transmission pattern

$$\mathbf{V}_{\text{hex}} = \begin{bmatrix} \frac{T}{2} & 0 \\ F & F \end{bmatrix} \quad (5)$$

which is named as *hexagonal multicarrier modulation* is illustrated in Figure 1.

For signal transmission with general transmission pattern  $\mathbf{V}_{\text{hex}}$ , the transmitted signal can be expressed as

$$\begin{aligned} s(t) &= \sum_z c_z g^\sigma(t, \mathbf{V}_{\text{hex}} \mathbf{z}) \\ &= \sum_m \sum_n c_{m,n} g^\sigma\left(t - m\frac{T}{2}, e^{j2\pi(m+2n)(F/2)t}\right), \end{aligned} \quad (6)$$

where  $g(t, \mathbf{V}_{\text{hex}} \mathbf{z})$  is the modulation pulse associated with  $c_z$ . The signaling efficiency can be easily calculated as  $\rho = 1/\sqrt{\det(\mathbf{V}_{\text{hex}}^T \mathbf{V}_{\text{hex}})} = 2/TF$ .

It is shown in [16] that the symbol energy perturbation function is dependent on the channel scattering function and the pulse shape. To optimally mitigate ISI/ICI caused by the mobile radio channels, the choices of modulation pulse and lattice generate matrix parameters should be matched to the maximum multipath delay spread and Doppler shift. The optimal system parameters for TF dispersive channels with exponential- $U$  scattering function can be chosen as [16]

$$\begin{aligned} \sigma &= \frac{W_t}{W_f} = \alpha \frac{\tau_{\text{rms}}}{f_d} = \sqrt{3} \frac{T}{F}, \\ \sigma &= \frac{W_t}{W_f} = \alpha \frac{\tau_{\text{rms}}}{f_d} = \frac{1}{\sqrt{3}} \frac{T}{F}. \end{aligned} \quad (7)$$

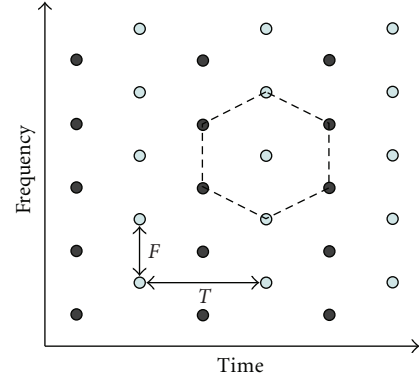


FIGURE 1: Partition of the hexagonal lattice into a rectangular sublattice  $\mathbf{V}_{\text{rect1}}$  (denoted by ●) and its coset  $\mathbf{V}_{\text{rect2}}$  (denoted by ○).

The baseband doubly dispersive channel can be modeled as a random linear operator  $H$ :

$$H[s(t)] = \int_0^{\tau_{\text{max}}} \int_{-f_d}^{f_d} H(\tau, \nu) s(t - \tau) e^{j2\pi\nu t} d\tau d\nu, \quad (8)$$

where  $H(\tau, \nu)$  is called the delay-Doppler spread function, which is the Fourier transform of the time-varying impulse response of the channel  $h(t, \tau)$  with respect to  $t$ . Moreover  $\tau_{\text{max}}$  and  $f_d$  are the maximum multipath delay spread and the maximum Doppler frequency, respectively. In wide-sense stationary uncorrelated scattering (WSSUS) assumption, the channel is characterized by the second-order statistics:

$$E[H(\tau, \nu) H^*(\tau_1, \nu_1)] = S_H(\tau, \nu) \delta(\tau - \tau_1) \delta(\nu - \nu_1), \quad (9)$$

where  $E[\cdot]$  denotes the expectation and  $S_H(\tau, \nu)$  is called the scattering function, which characterizes the statistics of the WSSUS channel. We assume that  $E[H(\tau, \nu)] = 0$ . Without loss of generality, we use  $\int_0^{\tau_{\text{max}}} \int_{-f_d}^{f_d} S_H(\tau, \nu) d\tau d\nu = 1$ , which means that the channel has no overall path loss.

It is shown in Figure 1 that the original hexagonal lattice can be expressed as the disjoint union of a rectangular sublattice  $\mathbf{V}_{\text{rect1}}$  and its coset  $\mathbf{V}_{\text{rect2}}$ . The transmitted signal (6) can be expressed as

$$\begin{aligned} s(t) &= \sum_m \sum_n \left[ c_{m,n}^1 g(t - mT) e^{j2\pi n F t} \right. \\ &\quad \left. + c_{m,n}^2 g\left(t - \left(m + \frac{1}{2}\right)T\right) e^{j2\pi(n+1/2)Ft} \right] \\ &= \sum_m \sum_n [c_{m,n}^1 g_{m,n}^1(t) + c_{m,n}^2 g_{m,n}^2(t)], \end{aligned} \quad (10)$$

where  $c_{m,n}^1$  and  $c_{m,n}^2$  represent the symbols coming from  $\mathbf{V}_{\text{rect1}}$  and  $\mathbf{V}_{\text{rect2}}$ , respectively.

The received signal is

$$r(t) = H[s(t)] + n(t), \quad (11)$$

where  $n(t)$  is the AWGN having variance  $\sigma_n^2$ . To obtain the data symbol  $\hat{c}_{m,n}^i$ , the receiver [2, 9, 10, 12, 13] projects on  $g_{m,n}^i(t)$ ,  $i = 1, 2$ , that is,

$$\begin{aligned}\hat{c}_{m,n}^i &= \langle r(t), g_{m,n}^i(t) \rangle \\ &= \langle H[s(t)], g_{m,n}^i(t) \rangle + \langle n(t), g_{m,n}^i(t) \rangle \\ &= \sum_j \sum_{m',n'} c_{m',n'}^j \langle H[g_{m',n'}^j(t)], g_{m,n}^i(t) \rangle + \langle n(t), g_{m,n}^i(t) \rangle.\end{aligned}\quad (12)$$

#### 4. Effects of Nonideal Transmission Conditions

Without loss of generality, we assume a timing offset  $\Delta t$  and carrier frequency offset  $\Delta f$ ; the received data symbol by using a projection receiver [2, 9, 10, 12, 13] can be expressed as

$$\begin{aligned}\hat{c}_{m,n}^i &= \langle e^{j2\pi\Delta f t} r(t), g_{m,n}^i(t - \Delta t) \rangle \\ &= \sum_{m',n'} c_{m',n'}^i \langle e^{j2\pi\Delta f t} H[g_{m',n'}^i(t)], g_{m,n}^i(t - \Delta t) \rangle \\ &\quad + \langle n(t), g_{m,n}^i(t - \Delta t) \rangle \\ &= \hat{c}_{m,n}^i \langle e^{j2\pi\Delta f t} H[g_{m,n}^i(t)], g_{m,n}^i(t - \Delta t) \rangle \\ \xi_{N+I} &\leftarrow \begin{cases} + \sum_{m' \neq m, n' \neq n} c_{m',n'}^i \langle e^{j2\pi\Delta f t} H[g_{m',n'}^i(t)], g_{m,n}^i(t - \Delta t) \rangle \\ + \sum_{m',n', j \neq i} c_{m',n'}^j \langle e^{j2\pi\Delta f t} H[g_{m',n'}^j(t)], g_{m,n}^i(t - \Delta t) \rangle \\ + \langle n(t), g_{m,n}^i(t - \Delta t) \rangle \end{cases} \\ &= e^{-j2\pi(\Delta f(m+(i-1)/2)T + (n+(i-1)/2)F\Delta t)} \\ &\quad \times c_{m,n}^i A_H(\tau_{\max}, f_d, \Delta t, \Delta f) + \xi_{N+I},\end{aligned}\quad (13)$$

where

$$\begin{aligned}A_H(\tau_{\max}, f_d, \Delta t, \Delta f) &= \int_0^{\tau_{\max}} \int_{-f_d}^{f_d} H(\tau, v) A_g^*(\tau + \Delta t, v + \Delta f) \\ &\quad \cdot e^{j2\pi v(m+(i-1)/2)T} e^{-j2\pi(n+(i-1)/2)F\tau} d\tau dv.\end{aligned}\quad (14)$$

The demodulated signal now consists of a useful portion and disturbances  $\xi_{N+I}$  caused by ISI, ICI, and AWGN. Concerning the useful portion, the transmitted symbols  $c_{m,n}^i$  are attenuated by  $A_H(\tau_{\max}, f_d, \Delta t, \Delta f)$  which is caused by doubly dispersive channel, timing offset, and carrier frequency offset. Meanwhile, the transmitted symbols rotated by a time-variant phasor

$$\phi = -j2\pi \left( \Delta f \left( m + \frac{(i-1)}{2} \right) T + \left( n + \frac{(i-1)}{2} \right) F \Delta t \right).\quad (15)$$

#### 5. Effects of TO, CFO, and DD Channels on SINR

The energy of received signal with TO and CFO over DD channels can be expressed as

$$\begin{aligned}E_r(\Delta t, \Delta f) &= E \left\{ \left| \sum_{m',n'} c_{m',n'}^i \langle e^{j2\pi\Delta f t} H[g_{m',n'}^i(t)], g_{m,n}^i(t - \Delta t) \rangle \right. \right. \\ &\quad \left. \left. + \langle n(t), g_{m,n}^i(t - \Delta t) \rangle \right|^2 \right\}.\end{aligned}\quad (16)$$

Using the assumption of transmitted symbols and the WSSUS channel, we get from (16) that

$$\begin{aligned}E_r(\Delta t, \Delta f) &= \sigma_c^2 \int_{\tau} \int_{\nu} S_H(\tau, \nu) \\ &\quad \times \left[ \sum_{m,n} \left( |A_g(mT + \tau - \Delta t, nF + \nu + \Delta f)|^2 \right. \right. \\ &\quad \left. \left. + \left| A_g \left( \left( m + \frac{1}{2} \right) T + \tau - \Delta t, \left( n + \frac{1}{2} \right) F + \nu + \Delta f \right) \right|^2 \right) \right] d\tau d\nu \\ &\quad + \sigma_n^2 |A_g(0, 0)|.\end{aligned}\quad (17)$$

Let  $E_s(\Delta t, \Delta f, \tau_{\text{rms}}, f_d)$  denote the signal energy

$$\begin{aligned}E_s(\Delta t, \Delta f, \tau_{\text{rms}}, f_d) &= \sigma_c^2 \int_{\tau} \int_{\nu} S_H(\tau, \nu) |A_g(\tau - \Delta t, \nu + \Delta f)|^2 d\tau d\nu.\end{aligned}\quad (18)$$

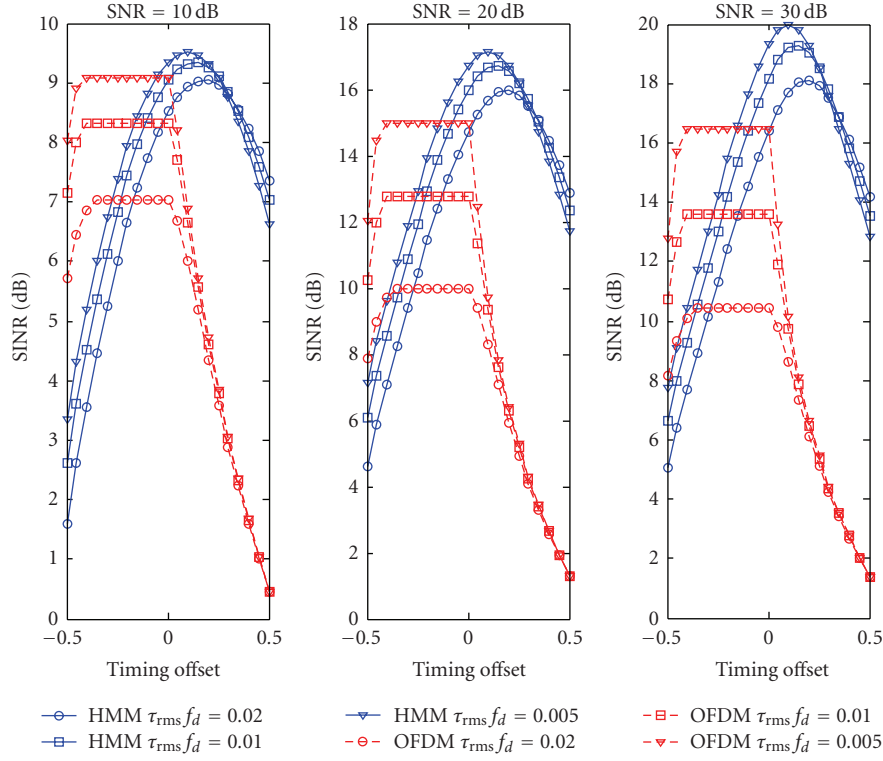
Moreover, let  $E_N(\Delta t, \Delta f, \tau_{\text{rms}}, f_d)$  denote the interference-plus-noise energy

$$\begin{aligned}E_N(\Delta t, \Delta f, \tau_{\text{rms}}, f_d) &= \sigma_c^2 \int_{\tau} \int_{\nu} S_H(\tau, \nu) \\ &\quad \times \left[ \sum_{z=[m,n]^T \neq [0,0]^T} \left( |A_g(mT + \tau - \Delta t, nF + \nu + \Delta f)|^2 \right. \right. \\ &\quad \left. \left. + \left| A_g \left( \left( m + \frac{1}{2} \right) T + \tau - \Delta t, \left( n + \frac{1}{2} \right) F \right. \right. \right. \\ &\quad \left. \left. \left. + \nu + \Delta f \right) \right|^2 \right) \right] d\tau d\nu + \sigma_n^2 |A_g(0, 0)|.\end{aligned}\quad (19)$$

We consider a DD channel with exponential delay power profile and U-shape Doppler power spectrum; the scattering function [21]

$$S_H(\tau, \nu) = \frac{1\sqrt{1 - (\nu/f_d)^2}}{(\tau_{\text{rms}}) e^{-\tau/\tau_{\text{rms}}} (1/\pi f_d)}\quad (20)$$

with  $\tau \geq 0$ ,  $|\nu| < f_d$ , where  $\tau_{\text{rms}}$  denotes the *rms delay spread* and  $f_d$  denotes the *maximal Doppler spread*.


 FIGURE 2: SINR for hexagonal multicarrier system for  $\Delta t \in [-0.5, 0.5]$ .

Upon substituting the scattering function (20) into (18) and (19), we have

$$E_s(\Delta t, \Delta f, \tau_{\text{rms}}, f_d) = \frac{\sigma_c^2}{\pi \tau_{\text{rms}} f_d} \int_0^\infty e^{-\tau/\tau_{\text{rms}}} e^{-(\pi/\sigma)(\tau-\Delta t)^2} d\tau \int_{-f_d}^{f_d} \frac{e^{-\sigma\pi(v+\Delta f)^2}}{\sqrt{1-(v/f_d)^2}} dv,$$

$$E_N(\Delta t, \Delta f, \tau_{\text{rms}}, f_d) = \frac{\sigma_c^2}{\pi \tau_{\text{rms}} f_d} \left\{ \sum_{(m,n) \neq (0,0)} \int_0^\infty e^{-\tau/\tau_{\text{rms}}} e^{-\pi(mT+\tau-\Delta t)^2/\sigma} d\tau \times \int_{-f_d}^{f_d} \frac{e^{-\sigma\pi(nF+v+\Delta f)^2}}{\sqrt{1-(v/f_d)^2}} dv + \sum_{(m,n) \neq (0,0)} \int_0^\infty e^{-\tau/\tau_{\text{rms}}} e^{-\pi((m+1/2)T+\tau-\Delta t)^2/\sigma} d\tau \times \int_{-f_d}^{f_d} \frac{e^{-\sigma\pi((n+1/2)F+v+\Delta f)^2}}{\sqrt{1-(v/f_d)^2}} dv \right\} + \sigma_n^2 |A_g(0,0)|. \quad (21)$$

SINR of received signal can be expressed as

$$R_{\text{SIN}}(\Delta t, \Delta f, \tau_{\text{rms}}, f_d) = \frac{E_s(\Delta t, \Delta f, \tau_{\text{rms}}, f_d)}{E_N(\Delta t, \Delta f, \tau_{\text{rms}}, f_d)}. \quad (22)$$

Plugging (21) into (22), we find

$$R_{\text{SIN}}(\Delta t, \Delta f, \tau_{\text{rms}}, f_d) = \frac{\sigma_c^2}{\pi \tau_{\text{rms}} f_d} \int_0^\infty e^{-\tau/\tau_{\text{rms}} - ((\pi/\sigma)(\tau-\Delta t)^2)} d\tau \int_{-f_d}^{f_d} \frac{e^{-\sigma\pi(v+\Delta f)^2}}{\sqrt{1-(v/f_d)^2}} dv \cdot \left( \frac{\sigma_c^2}{\pi \tau_{\text{rms}} f_d} \left\{ \sum_{(m,n) \neq (0,0)} \int_0^\infty e^{-\tau/\tau_{\text{rms}} - (\pi(mT+\tau-\Delta t)^2/\sigma)} d\tau \times \int_{-f_d}^{f_d} \frac{e^{-\sigma\pi(nF+v+\Delta f)^2}}{\sqrt{1-(v/f_d)^2}} dv + \sum_{(m,n) \neq (0,0)} \int_0^\infty e^{-\tau/\tau_{\text{rms}} - (\pi((m+1/2)T+\tau-\Delta t)^2/\sigma)} d\tau \times \int_{-f_d}^{f_d} \frac{e^{-\sigma\pi((n+1/2)F+v+\Delta f)^2}}{\sqrt{1-(v/f_d)^2}} dv \right\} + \sigma_n^2 |A_g(0,0)| \right)^{-1}. \quad (23)$$

Equation (23) indicates that  $R_{\text{SIN}}(\Delta t, \Delta f, \tau_{\text{rms}}, f_d)$  can be modeled as a function of CFO, TO, and channel spread factor  $\tau_{\text{rms}} f_d$ .

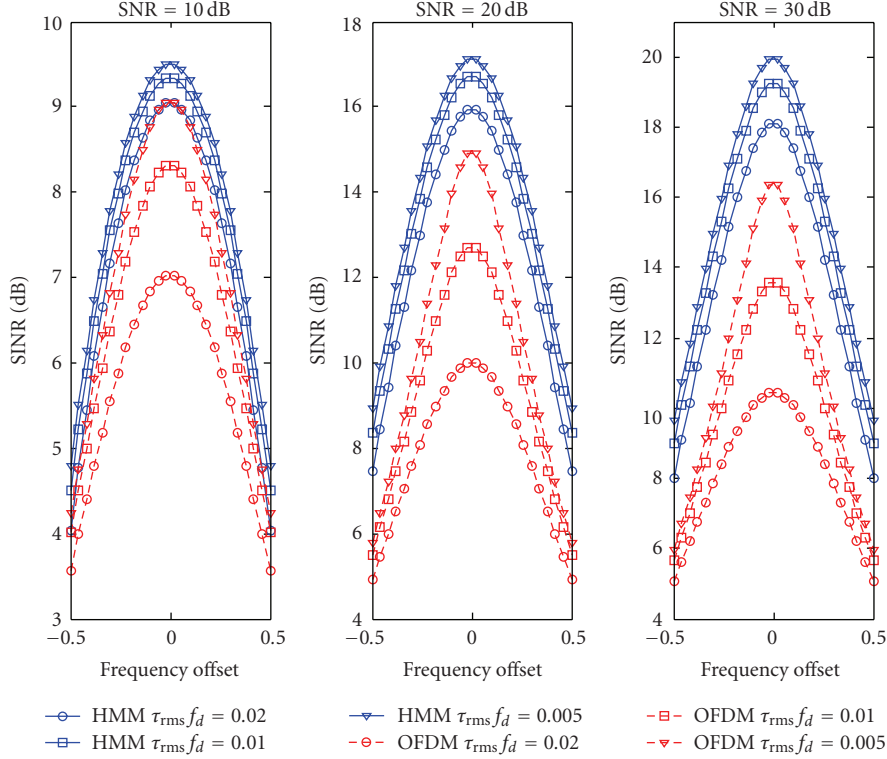


FIGURE 3: SINR for hexagonal multicarrier system for  $\Delta f \in [-0.5, 0.5]$ .

## 6. Numerical Results and Discussion

Here, we examine the SINR performance of hexagonal multicarrier systems over a DD channel. All experiments employed  $N = 80$ ,  $\sigma = T/\sqrt{3}F$  hexagonal multicarrier system, and  $\tau_{\text{rms}}/f_d$  of DD channel is fixed. Obviously, the hexagonal transmission pattern is fixed while the rms delay spread and the maximal Doppler spread increase simultaneously with the increasing of channel spread factor  $\tau_{\text{rms}}f_d$ . The center carrier frequency is set to  $f_c = 5$  GHz and the sampling intervals  $T_s = 10^{-6}$  s,  $F = 25$  kHz, and  $T = 1 \times 10^{-4}$  s.  $\Delta t$  in all simulation results are normalized to  $T/2$ , and  $\Delta f$  are normalized to  $F/2$ .

We fixed  $\Delta f$  to 0 and the product  $\tau_{\text{rms}}f_d$  to 0.02, 0.01, and 0.005. We repeat this simulation for a variety of values SNR in the range of 10 dB ~ 30 dB. The result is shown in Figure 2. We see that the power of the ISI and ICI caused by TO strongly depends on the channel spread factor of DD channel. The maximum SINR timing decreases with the product  $\tau_{\text{rms}}f_d$  increasing, and the timing offset  $\Delta t$  increases as the product  $\tau_{\text{rms}}f_d$  increases, that is, there is a delay between the maximum SINR timing and the first tap of DD channel from the SINR point of view. It can be seen from Figure 2 that the aforementioned delay increases as the product  $\tau_{\text{rms}}f_d$  increases. HMM does an excellent job of maintaining high SINR. CP-OFDM with guard  $N_g = N/4$  perfectly suppresses ISI caused by TO within cyclic prefix, but does a poor job of combating the DD channel, and there is an SINR gap between HMM and CP-OFDM about 4 ~ 7 dB at SNR = 30 dB.

In Figure 3, we fixed  $\Delta t$  to the maximum SINR timing and the product  $\tau_{\text{rms}}f_d$  to 0.02, 0.01, and 0.005. It is seen that the SINR depends on the channel spread factor of DD channel and the SINR obtains its maximum value at  $\Delta f$ . Meanwhile, SINR decreases with the product  $\tau_{\text{rms}}f_d$  increasing. From Figure 3, we see that HMM also does a good job of ISI/ICI suppression, and there is also an SINR gap between HMM and CP-OFDM about 4 ~ 8 dB at SNR = 30 dB and CFO in the range of  $-0.5 \sim 0.5$ . Effects of both CFO and TO on the SINR performance of hexagonal multicarrier systems and CP-OFDM systems at SNR = 30 dB are shown in Figure 4,  $\tau_{\text{rms}}f_d$  is set to 0.02.

The maximum SINR with the variety of SNR and  $\tau_{\text{rms}}f_d$  is depicted in Figure 5. A lower bound (LB) on the effects of Doppler spread in SINR performance of OFDM system [18] is depicted for comparison. It can be seen that there is a degradation of SINR with the increasing of  $\tau_{\text{rms}}f_d$ . There is about 1 dB SINR loss of HMM system with  $\tau_{\text{rms}}f_d$  from 0.01 to 0.02 while OFDM SINR loss is about 3 dB. HMM system does a good job of combating DD channel. The degradation of SINR in CP-OFDM system increases as the channel spread factor increases.

## 7. Conclusion

This paper examines the effects of insufficient synchronization on the amplitude and phase of the demodulated symbol by using a projection receiver in hexagonal multicarrier modulation systems. Furthermore, effects of CFO, TO, and

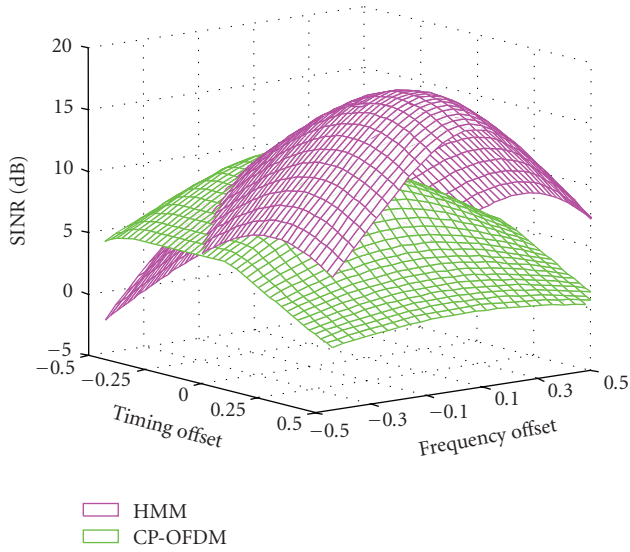


FIGURE 4: Effects of TO and CFO on SINR for hexagonal multicarrier system with  $\tau_{rms} f_d = 0.02$  at SNR = 30 dB.

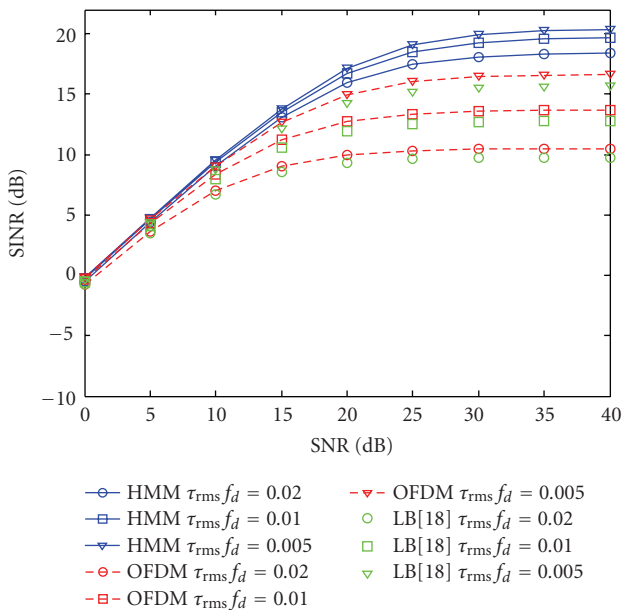


FIGURE 5: Effects of channel spread factor on SINR for hexagonal multicarrier system.

channel spread factor on the performance of SINR in hexagonal multicarrier modulation systems are further discussed. The exact SINR expression versus insufficient synchronization and channel spread factor is derived. Both theoretical analysis and simulation results show that similar degradation on symbol amplitude and phase caused by insufficient synchronization is incurred as in common OFDM transmission: (1) CFO and TO introduce interference among subcarriers and symbols; (2) the transmitted symbols experience an amplitude reduction and a time variant phase shift due to CFO; (3) the transmitted symbols are attenuated and rotated by a phasor whose phase is proportional to the subcarrier

index and TO; (4) the SINR of received symbols decreases as the channel spread factor increases. Our theoretical analysis is confirmed by numerical simulations, showing that HMM systems outperform traditional CP-OFDM systems with respect to SINR against ISI/ICI caused by insufficient synchronization and doubly dispersive channel.

**Acknowledgment**

This research was supported by China National Science Fund under Contract no. 60772083.

**References**

- [1] T. S. Rappaport, A. Annamalai, R. M. Buehrer, and W. H. Tranter, "Wireless communications: past events and a future perspective," *IEEE Communications Magazine*, vol. 40, no. 5, pp. 148–161, 2002.
- [2] W. Kozek and A. F. Molisch, "Nonorthogonal pulseshapes for multicarrier communications in doubly dispersive channels," *IEEE Journal on Selected Areas in Communications*, vol. 16, no. 8, pp. 1579–1589, 1998.
- [3] D. Schaffhuber, G. Matz, and F. Hlawatsch, "Pulse-shaping OFDM/BFDM systems for time-varying channels: ISI/ICI analysis, optimal pulse design, and efficient implementation," in *Proceedings of the 13th IEEE International Symposium on Personal, Indoor and Mobile Radio Communications (PIMRC '02)*, vol. 3, pp. 1012–1016, Lisbon, Portugal, September 2002.
- [4] R. Haas and J.-C. Belfiore, "A time-frequency well-localized pulse for multiple carrier transmission," *Wireless Personal Communications*, vol. 5, no. 1, pp. 1–18, 1997.
- [5] B. Le Floch, M. Alard, and C. Berrou, "Coded orthogonal frequency division multiplex [TV broadcasting]," *Proceedings of the IEEE*, vol. 83, no. 6, pp. 982–996, 1995.
- [6] H. Bölcskei, P. Duhamel, and R. Hleiss, "Design of pulse shaping OFDM/OQAM systems for high data-rate transmission over wireless channels," in *Proceedings of the IEEE International Conference on Communications (ICC '99)*, vol. 1, pp. 559–564, Vancouver, Canada, June 1999.
- [7] S. Mirabbasi and K. Martin, "Overlapped complex-modulated transmultiplexer filters with simplified design and superior stopbands," *IEEE Transactions on Circuits and Systems II*, vol. 50, no. 8, pp. 456–469, 2003.
- [8] P. Martin, F. Cruz-Roldan, and T. Saramaki, "A windowing approach for designing critically sampled nearly perfect-reconstruction cosine-modulated transmultiplexers and filter banks," in *Proceedings of the 3rd International Symposium on Image and Signal Processing and Analysis (ISPA '03)*, vol. 2, pp. 755–760, Rome, Italy, September 2003.
- [9] T. Strohmer and S. Beaver, "Optimal OFDM design for time-frequency dispersive channels," *IEEE Transactions on Communications*, vol. 51, no. 7, pp. 1111–1122, 2003.
- [10] K. Liu, T. Kadous, and A. M. Sayeed, "Orthogonal time-frequency signaling over doubly dispersive channels," *IEEE Transactions on Information Theory*, vol. 50, no. 11, pp. 2583–2603, 2004.
- [11] V. Kumbasar and O. Kucur, "ICI reduction in OFDM systems by using improved sinc power pulse," *Digital Signal Processing*, vol. 17, no. 6, pp. 997–1006, 2007.

- [12] P. Jung and G. Wunder, "The WSSUS pulse design problem in multicarrier transmission," *IEEE Transactions on Communications*, vol. 55, no. 10, pp. 1918–1928, 2007.
- [13] S. Das and P. Schniter, "Max-SINR ISI/ICI-shaping multicarrier communication over the doubly dispersive channel," *IEEE Transactions on Signal Processing*, vol. 55, no. 12, pp. 5782–5795, 2007.
- [14] M. Ma, B. Jiao, and W. C. Y. Lee, "A dual-window technique for enhancing robustness of OFDM against frequency offset," *IEEE Communications Letters*, vol. 12, no. 1, pp. 17–19, 2008.
- [15] G. Lin, L. Lundheim, and N. Holte, "Optimal pulses robust to carrier frequency offset for OFDM/QAM systems," *IEEE Communications Letters*, vol. 12, no. 3, pp. 161–163, 2008.
- [16] F.-M. Han and X.-D. Zhang, "Hexagonal multicarrier modulation: a robust transmission scheme for time-frequency dispersive channels," *IEEE Transactions on Signal Processing*, vol. 55, no. 5, part 1, pp. 1955–1961, 2007.
- [17] P. Jung and G. Wunder, "On time-variant distortions in multicarrier transmission with application to frequency offsets and phase noise," *IEEE Transactions on Communications*, vol. 53, no. 9, pp. 1561–1570, 2005.
- [18] X. Cai and G. B. Giannakis, "Bounding performance and suppressing intercarrier interference in wireless mobile OFDM," *IEEE Transactions on Communications*, vol. 51, no. 12, pp. 2047–2056, 2003.
- [19] J. H. Conway and N. J. A. Sloane, *Sphere Packings, Lattices and Groups*, Springer, New York, NY, USA, 2nd edition, 1993.
- [20] L. Cohen, *Time-Frequency Analysis*, Prentice-Hall, Englewood Cliffs, NJ, USA, 1995.
- [21] M. Pätzold, *Mobile Fading Channels*, John Wiley & Sons, West Sussex, UK, 2002.